

Conclusions

The macro-parametric method for exchanging parametric information of a CAD model of MEMS sensors for integration of heterogeneous CAD systems is developed that allowed to increase design efficiency. The structure of the integrated design subsystem and client-side software for MEMS motion sensors are developed based on the proposed macro-parametric method.

1. Колчин А. Ф. Управление жизненным циклом продукции / А. Ф. Колчин, М. В. Овсянников, А. Ф. Стрекалов, С. В. Сумароков. – М.: Анахарсис, 2002. 2. Лобур М. В. Дослідження параметрів стратегії автоматичного трасування в САПР PCAD / М. В. Лобур, Р. Т. Панчак, З. Ю. Готра, В. В. Григор'єв // Вісник Державного університету "Львівська політехніка": Комп'ютерні системи проектування. Теорія і практика. – Львів, 2000. 3. Reddy Y.V., Ramana. Srinivas, Kanakanahalli, Jagannathan, V. Karinithi, Raghu. Computer support for concurrent engineering, Computer, V26. – P12(4). – Jan, 1993. 4. Three Dimensional CAD Interface Specification for Electro-Mechanical Collaborative Design Using ISO 10303-210, ME009.01.00, 27 February 2001, PDES, Inc: <http://pdesinc.aticorp.org>. 5. CIMS-ERC.CE Project Final Report, China CIMS-ERC Technical Report. 1997-12. 6. CE'96/ISPE. The Proceedings of the Concurrent Engineering Research and Application. – Toronto University, Canada, 1996-08. 7. Dwivedi. Concurrent Engineering – An Introduction / Dwivedi, Suren N. and Sobolewski Michael // Proc. of the Vth Intern. Conf. on CAD/CAM Robotics and Factories of the Future '90. – Vol. 1: Concurrent Engineering. – New York: Springer-Verlag, 1991. – P. 3–16. 8. Nevins J.L., Whitney D.E. Concurrent Design of Products and Processes. – McGraw-Hill, New York, 1989. – 268 p.

UDK 519.6:621.396

M. I. Andriychuk

Pidstryhach Institute for Applied Problems in Mechanics and Mathematics, NASU,
Lviv Polytechnic National University
CAD Department

NON-DESTRUCTIVE TESTING OF MATERIALS BASED ON THE WAVE SCATTERING BY THE SMALL PARTICLES

© Andriychuk M. I., 2012

The theory of scattering of the acoustic waves on the small bodies is applied to solution of problem related to the non-destructive testing of materials with defects. The change of the refraction coefficient of the acoustic wave passing through the steel pattern testifies to presence of microdefects in material. The numerical results are presented for several kinds of steel and they confirm the possibility to apply the asymptotic scattering theory to problems of the non-destructive testing.

Key words: scattering, small bodies, microdefects, non-destructive testing.

Теорія розсіяння акустичних хвиль на малих тілах використовується для розв'язання задачі, пов'язаної з неруйнівним контролем матеріалів з дефектами. Зміна коефіцієнта заломлення акустичної хвилі, яка проходить крізь сталевий зразок, свідчить про наявність мікродефектів у ньому. Числові результати наведено для декількох видів сталі; вони свідчать про можливість застосовувати теорію асимптотичного розсіяння до задач неруйнівного контролю.

Ключові слова: розсіяння, малі тіла, мікродефекти, неруйнівний контроль.

Introduction

The presence and evolution of micro-defects in materials and structures is prevailing cause of their destruction. Microdefects reduce the residual life of production and objects that cause a threat of accidents and failures. Therefore, early diagnostics and identification of degree of the material damage and the nature

of microdefects allow to prevent such situations in the future, to improve the technological safety, and assess their remaining life. Timely detection of microdamages is especially necessary while the non-destructive testing of thermal power equipment such as steam pipes that is exposed to high temperatures and pressures during operation.

To assess the state of changing the investigated material, the examination of structure of the acoustic field for waves passing through the sample, with varying degrees microdamages, is used. It is obvious that the structure of this field contains information about the microdefects in the material, and the goal of researchers is to develop methods for processing acoustic signals, what allows to allocate this information. Least frequently, the Doppler laser interferometer OFV5000 produced by GmbH "Polytec" [1] is applied for obtaining the dependencies of the normal component of particle velocity with time at various points in the surface of samples.

An asymptotic approach to solving the problems of wave scattering on a set of small particles, elaborated by A. G. Ramm in [2]-[6], is the theoretical basis for the studying the characteristics of an acoustic wave passing through a medium containing microdefects. This approach allows to determine a refractive index of the acoustic wave passing through a medium containing microdefects. In turn, this allows to define a wavelength in the defective material, and hence the normal component of particle velocity can be calculated [7].

An asymptotically exact solution of the many-body wave scattering problem was developed in [4] under the assumptions $ka \ll 1$, $d = O(a^{1/3})$, $M = O(1/a)$, where a is the size of the particles, $k = 2\pi / l$ is the wave number, d is the distance between neighboring particles, and M is the total number of the particles contained in the bounded domain $D \subset \mathbb{R}^3$ (see Fig. 1). An impedance boundary condition on the boundary S_m of the m -th inclusion (particle) D_m was assumed. In [5], the above assumptions were generalized as:

$$z_m = \frac{h(x_m)}{a^k}, \quad d = O(a^{(2-k)/3}), \quad M = O\left(\frac{1}{a^{2-k}}\right), \quad k \in (0,1), \quad (1)$$

where z_m is the boundary impedance, $h_m = h(x_m)$, $x_m \in D_m$, and $h(x) \in C(D)$ is an arbitrary continuous in \bar{D} function, $\text{Im} h \leq 0$.

The initial field u_0 satisfies the Helmholtz equation in \mathbb{R}^3 and the scattered field satisfies the radiation condition. Let the small particle D_m be a ball of radius a centered at the point x_m , $1 \leq m \leq M$.

Solution of scattering problem

The scattering problem consists in solution of the Helmholtz equation supplemented by the respective boundary conditions:

$$[\nabla^2 + k^2 n_0^2(x)]u_M = 0 \quad \text{in } \mathbb{R}^3 \setminus \bigcup_{m=1}^M D_m, \quad (2)$$

$$\frac{\partial u_M}{\partial N} = z_m u_M \quad \text{on } S_m, \quad 1 \leq m \leq M, \quad (3)$$

where

$$u_M = u_0 + v_M, \quad (4)$$

u_0 is solution to (2), (3) with $M = 0$, (i.e. in the absence of embedded particles) and with the incident field e^{ikax} , and v_M satisfies the radiation conditions.

The unique solution to (2) – (4) is of the form

$$u_M(x) = u_0(x) + \sum_{m=1}^M \int_{S_m} G(x,y) \mathcal{S}_m(y) dy, \quad (5)$$

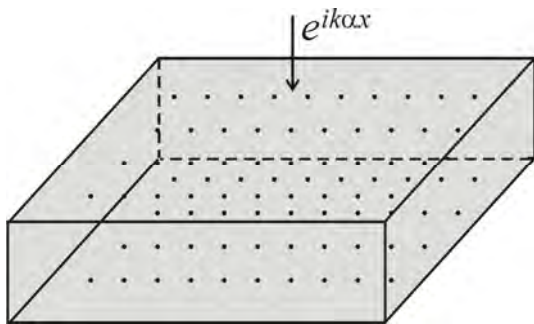


Fig. 1. Geometry of problem

where $G(x, y)$ is Green's function of Helmholtz equation in the case when $M = 0$.

Let us introduce the "effective field" u_e , acting on the m -th particle:

$$u_e(x) := u_e(x, a) := u_e^{(m)}(x) := u_M(x) - \int_{S_m} G(x, y) \mathcal{S}_m(y) dy, \quad x \in \mathbb{R}^3. \quad (6)$$

Let $\Delta_p \subset D$ be any subdomain of D , and $N(\Delta_p)$ be the number of particles in Δ_p . We assume that

$$N(\Delta_p) = \frac{1}{a^{2-k}} \int_{\Delta_p} N(x) dx [1 + o(1)], \quad a \rightarrow 0, \quad (7)$$

where $N(x) \geq 0$ is a given continuous function in D . It was proved in [5] that

$$\lim_{a \rightarrow 0} \|u_e(x) - u(x)\|_{C(D)} = 0, \quad (8)$$

and $u(x)$ solves the following equation:

$$u(x) = u_0(x) - 4p \int_D G(x, y) h(y) N(y) u(y) dy. \quad (9)$$

Formula (9) presents the equation for the limiting effective field in the medium, created by embedding many small particles with the distribution law (7).

Approximate solution for effective field

Let us derive an explicit formula for the effective field u_e . Rewrite the exact formula (5) as:

$$u_M(x) = u_0(x) + \sum_{m=1}^M G(x, x_m) Q_m + \sum_{m=1}^M \int_{S_m} [G(x, y) - G(x, x_m)] \mathcal{S}_m(y) dy, \quad (10)$$

where $Q_m = Q_m(\mathcal{S}_m)$.

Using some estimates of $G(x, y)$ [4] and the asymptotic formula for Q_m from [5], we can rewrite the exact formula (10) as follows:

$$u_M(x) = u_0(x) + \sum_{m=1}^M G(x, x_m) Q_m + o(1), \quad a \rightarrow 0, \quad |x - x_m| \geq a. \quad (11)$$

The number $Q_m(x)$ is given by the asymptotic formula

$$Q_m = -4p h(x_m) u_e(x_m) a^{2-k} [1 + o(1)], \quad a \rightarrow 0, \quad (12)$$

and the asymptotic formula for \mathcal{S}_m is

$$\mathcal{S}_m = -\frac{h(x_m) u_e(x_m)}{a^k} [1 + o(1)], \quad a \rightarrow 0. \quad (13)$$

Finally, formula for $u_e(x)$ is given by

$$u_e^{(j)}(x) = u_0(x) - 4p \sum_{m=1, m \neq j}^M G(x, x_m) h(x_m) u_e(x_m) a^{2-k} [1 + o(1)]. \quad (14)$$

Equation (9) for the limiting effective field $u(x)$ is used in numerical calculations.

The numerical calculation of the field u_e by formula (14) requires the knowledge of the numbers $u_m := u_e(x_m)$. These numbers are obtained by solving a linear algebraic system (LAS). This system is

$$u_j = u_{0j} - 4p \sum_{m=1, m \neq j}^M G(x_j, x_m) h(x_m) u_m a^{2-k}, \quad j = 1, 2, \dots, M. \quad (15)$$

This LAS is convenient for numerical calculations, because its matrix is often diagonally dominant.

On the other hand, for finding the solution to the limiting equation (9), we use the collocation method from [6], which yields the following LAS:

$$u_j = u_{0j} - 4p \sum_{p=1, p \neq j}^P G(x_j, x_p) h(y_p) N(y_p) u_p |\Delta_p|, \quad p = 1, 2, \dots, P, \quad (16)$$

where P is number of small cubes Δ_p , y_p is center of Δ_p , $|\Delta_p|$ is volume of Δ_p . We assume that the union of Δ_p forms a partition of D , and the diameter of Δ_p is $O(d^{1/2})$.

From the computational point of view solving LAS (16) is much easier than LAS (15), because $P \ll M$.

We have two different LAS, corresponding to formula (14) and to equation (9). Solving these LAS, one can compare their solutions and evaluate the limits of applicability of the asymptotic approach from [5] to solving many-body wave scattering problem in the case of small particles.

Numerical simulation

The numerical approach to solve the wave scattering problem for small particles was developed in [8]. Some numerical results, which confirmed the applicability of the asymptotic approach to solution of many-body wave scattering problem, were received there.

From the practical point of view, the following numerical experiments are important:

a) to investigate the relative difference between solutions to the limiting equation (9) and the LAS (16);

b) for large M , say, $M = 10^5$, $M = 10^6$, to investigate the relative difference between solutions to the limiting equation (9) and the LAS (15);

c) to investigate of the relative difference between solutions to LAS (15) and LAS (16);

d) using method [5] for creating materials with desired refraction coefficient to investigate the change of $n^2(x)$ and length of acoustic wave depending on the number of the small particles (defects) contained in a pattern.

The calculation a)-c) allow to ascertain the limits of applicability of the asymptotic approach and determine the range of physical parameters of problem for which the proposed approach can simulate the propagation of acoustic waves in the patterns under investigation. The calculations related to item d) allow to assess the changing the refraction coefficient and length of the acoustic wave in the defect media and explain the non-linear character of wave's length change while the increasing the number of defects (see [7]).

The recipe to calculate the refraction coefficient $n^2(x)$ of media having the small inclusions was proposed in [5]. The computational formula was derived in [9]:

$$n^2(x) = -\frac{4\rho h(x)N}{k^2} + n_0^2, \quad (17)$$

where n_0^2 is refraction coefficient of initial media (without the defects), parameter N is determined as

$$N = \frac{Ma^{2-k}}{V}, \quad (18)$$

M is quantity of particles in the given domain D , V is volume of D . Function $h(x)$ is given by

$$h(x) = za^{2-k}, \quad (19)$$

where z is the acoustic impedance.

The calculations related to items a)-c) are presented in Figs. 2-9.

Relative difference between solutions to the limiting equation (9) and the LAS (16). The numerical procedure for checking the accuracy of the solution to equation (9) uses the calculations with various values of the parameters k , a , l_D , and $h(x)$, where l_D is diameter of D . The absolute and relative errors were calculated by increasing the number of collocation points. The dependence of the accuracy on the parameter, where $\rho = \sqrt[3]{P}$, P is the total number of small subdomains in D , is shown in Fig. 2 and Fig. 3 for $k=1.0$, $l_D=0.5$, $a=0.01$ at the different values of $h(x)$. The solution corresponding to $\rho=20$ is considered as "exact" solution (the number P for this case is equal to 8000).

The error of the solution to equation (9) is equal to 1.1 % and 0.02 % for real and imaginary part, respectively, at $\rho=5$ (125 collocation points), it decreases to values of 0.7 % and 0.05 % if $\rho=6$ (216 collocation points), and it decreases to values 0.29 % and 0.02 % if $\rho=8$ (512 collocation points), $h(x) = k^2(1-3i)/(40\pi)$. The relative error smaller than 0.01 % for the real part of solution is obtained at

$\rho = 12$, this error tends to zero when ρ increases. This error depends on the function $h(x)$ as well, it diminishes when the imaginary part of $h(x)$ decreases. The error for the real and imaginary parts of the solution at $\rho = 19$ does not exceed 0.006 %.

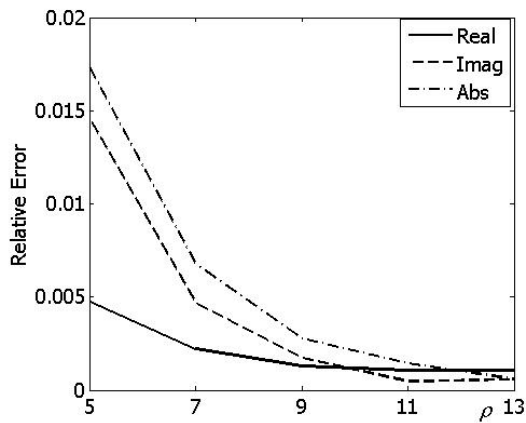


Fig. 2. Relative error versus the parameter r ,
 $h(x) = k^2(1-7i)/(40p)$

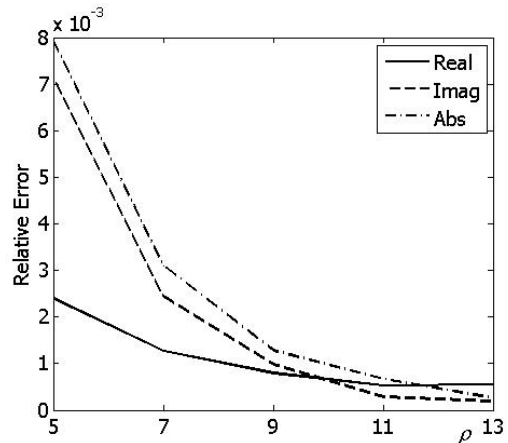


Fig. 3. Relative error versus the parameter r ,
 $h(x) = k^2(1-3i)/(40p)$

The numerical calculations show that the error depends much on the value of k . In Fig. 4 and Fig. 5, the results are shown for $k = 2.0$ and $k = 0.6$, respectively ($h(x) = k^2(1-3i)/(40\pi)$). It is seen that the error is nearly 10 times larger at $k = 2.0$. The maximal error (at $\rho = 5$) for $k = 0.6$ is less than 30 % of the error for $k = 1.0$. This error tends to zero even faster for smaller k .

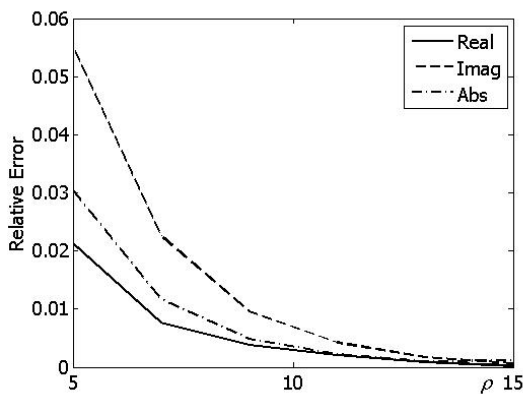


Fig. 4. Relative error versus the parameter r , $k = 2.0$

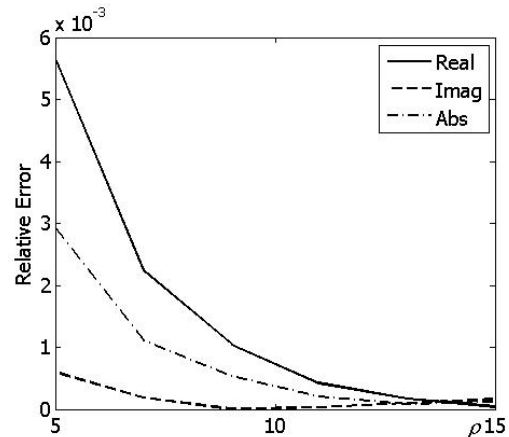


Fig. 5. Relative error versus the parameter r , $k = 0.6$

Relative difference between solutions to the limiting equation (9) and LAS (15). As before, we consider as the “exact” solution to (9) the approximate solution to LAS (17) with $\rho = 20$. The maximal relative error for such ρ does not exceed 0.01 % in the range of problem parameters we have considered ($k = 0.5 \div 1.0$, $l_D = 0.5 \div 1.0$, $N(x) \geq 4.0$). The numerical calculations are carried out for various sizes of the domain D and various function $N(x)$.

The results for big values of M are presented in Table 1 for $k = 1.0$, $N(x) = 40.0$, and $l_D = 1.0$. The second line contains the values of a_{est} , the estimated value of a , calculated by formula (7), with the number $N(\Delta_p)$ replacing the number M . In this case the radius of a particle is calculated as

$$a_{est} = (M / \int_{\Delta_p} N(x) dx)^{1/(2-\kappa)}$$

The values of a_{opt} in the third line correspond to optimal values of a , which yield minimal relative error of the modulus of the solutions to equation (9) and LAS (16). The fourth line contains the values of the distance d between particles. The maximal value of the error is obtained when $\mu = 7$, $\mu = \sqrt[3]{M}$ and it decreases slowly when μ increases. The minimal error of the solutions is obtained at $\mu = 60$ (total number of particles $M = 2.16 \times 10^5$).

Table 1

Optimal parameters of D for big μ , $N(x) = 40.0$

μ	20	30	40	50	60
a_{est}	0.0081	0.0027	0.0012	6.65×10^{-4}	4.04×10^{-4}
a_{opt}	0.0077	0.0025	0.0011	6.61×10^{-4}	4.04×10^{-4}
d	0.0526	0.0345	0.0256	0.0204	0.0169
Rel. Error	0.59 %	0.35 %	0.36 %	0.27 %	0.19 %

The relative error of the solution to LAS (15) tends to the relative error of the solution to LAS (16) when the parameter μ becomes greater than 80 ($M = 5.12 \times 10^5$). The relative error of the solution to LAS (16) is calculated by taking the norm of the difference of the solutions to (16) with P and $2P$ points, and dividing it by the norm of the solution to (16) calculated for $2P$ points. The relative error of the solution to LAS (16) is calculated by taking the norm of the difference between the solution to (15), calculated by an interpolation formula at the points y_p from (16), and the solution of (16), and dividing the norm of this difference by the norm of the solution to (16).

Relative difference between solutions to LAS (15) and LAS (16). The solution to LAS (16) is considered as benchmark solution; at $P = 8000$, the relative error of solution to LAS (16) does not exceed 0.01%. The number of defects M is equal to 192. In Fig. 6, the dependence of the relative error on the distance d between particles is shown; one can see that minimal error is attained at $d \sim 4a - 5a$ for real (solid line) and imaginary (dashed line) parts of solution (it is equal to 2.3% and 0.94% respectively), the minimal error for module (dot-dashed line) of solution is attained at $d \sim 8a$ and it is equal to 0.09%. The respective error for particles with radius $a = 0.005$ are equal to 1.7%, 0.59%, and 0.01%, respectively, (see Fig. 7). The values of optimal d are shifted to the left in comparison with Fig. 6; the both parameters a and d are given in the relative units.

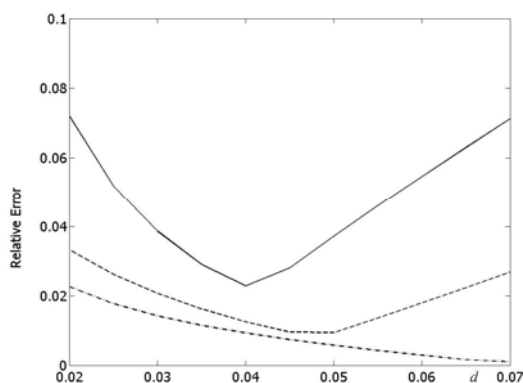


Fig. 6. Relative error of solution to LAS (15) versus distance d between defects, $a = 0.01$, $M = 192$

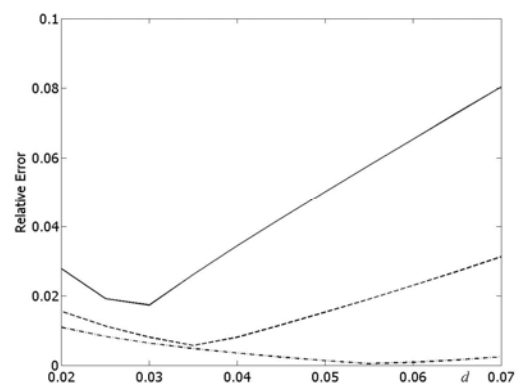


Fig. 7. Relative error of solution to LAS (15) versus distance d between defects, $a = 0.005$, $M = 192$

The calculations with bigger number of defects are shown in Figs. 8-9. The relative error for this case grows slowly. The optimal values of d are shifted to right in comparison with Figs. 6-7, and the

minimal values of error for $a=0.01$ are equal to 2.7 %, 1.3 % and 0.2 % for the real part, imaginary part and module of solution. At $a=0.005$, the minimal errors amount 1.9 %, 0.7 % and 0.1 %, respectively.

Numerical calculations for wider range of the distance d demonstrate that there is an optimal value of d , starting from which the deviation of solutions increases again. These optimal values of d are shown in Table 2 for various $N(x)$. The calculations show that the optimal distance between particles increases when the number of particles grows. For the number of particles $M=15^3$, i.e. $\mu=15$, this distance is about $10a$.

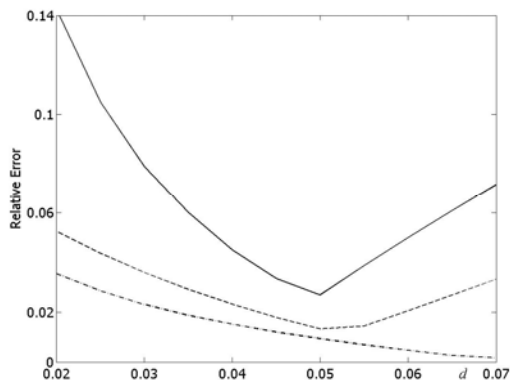


Fig. 8. Relative error of solution to LAS (15) versus distance d between defects, $a=0.01$, $M=480$

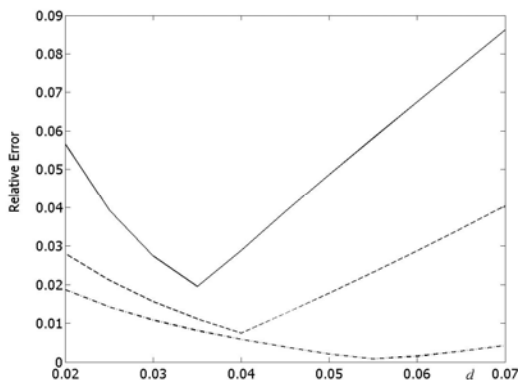


Fig. 9. Relative error of solution to LAS (15) versus distance d between defects, $a=0.005$, $M=480$

Table 2

Optimal values of d for various $N(x)$

$N(x)$	$N(x)=10$	$N(x)=20$	$N(x)=30$	$N(x)=40$	$N(x)=50$
$a=0.001$	0.08835	0.07678	0.06331	0.06317	0.05056
$a=0.005$	0.07065	0.04724	0.04716	0.04709	0.04122

Change of refraction coefficient depending on the number of defects contained in a pattern.

The investigation of change of the refraction coefficient n^2 for the case of metal pattern is carried out by the example of steel plate containing the microdefects thick with air. The parameters of problems are the following: the speed of sound in air is equal to $340m/s$, the speed of sound in steel is equal to $5130m/s$, acoustic impedance Z of air is equal to $420Pa \cdot s/m$, the wave number $k=10^4m^{-1}$, the refraction coefficient n_0^2 for steel is equal to 15.0882^2 . The radius of particles is given in mm (micrometers).

In order to investigate the dependence of resulting refraction coefficient $n^2(x)$ on the parameters of pattern, it is more convenient to give formula (17) by

$$n^2 = -\frac{4pz}{k^2 s^3 a} + n_0^2, \quad (20)$$

where s is the parameter determinative the distance d between the particles (defects), $d=sa$. It is assumed in the presented calculations that the defects are distributed uniformly in D , and the value of n^2 does not depend on the coordinate $x=(x_1, x_2, x_3)$. The results presented in Fig. 10 show that the refraction coefficient n^2 tends to the refraction coefficient n_0^2 of initial media (without defects) if the distance between the particles grows, the dependence of n^2 on the radius a of particles is non-monotone (the values of n are shown in Figs. 10, 11). Of course, the formulas (17) and (20) for the case of non-uniformly

distribution of particles, their different radius, and dependence of the acoustic impedance on the coordinate x is more complicate.

The results explanatory the variation of refraction coefficient n^2 in the range $a = 10^{-7} - 10^{-6}$ for various s are shown in Fig. 11. Similarly to Fig. 10, the refraction coefficient n^2 tends to the refraction coefficient n_0^2 of media without the defects, if the distance between defects grows. Similar properties of n^2 are observed for others values of a . The difference between n^2 and n_0^2 grows if the radius a of particle increases, the difference depends on a non-monotonically.

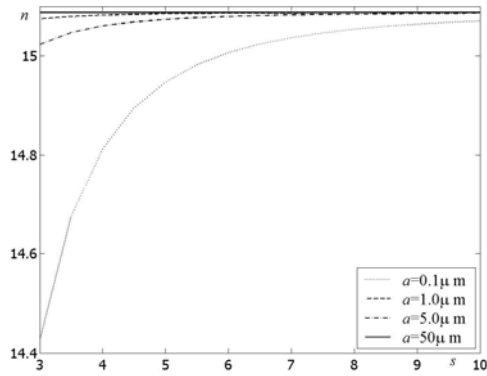


Fig. 10. The values of n versus the parameter s in formula (20)

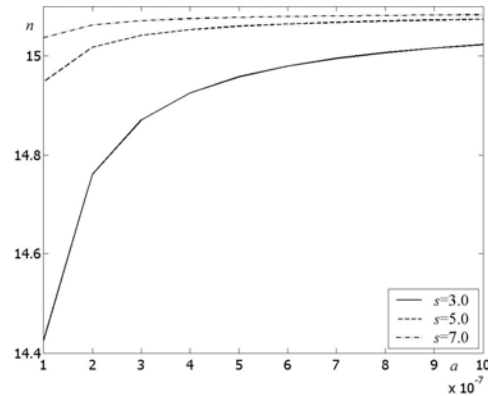


Fig. 11. The values of n versus the radius a of defect

Conclusions

The numerical results based on the asymptotical approach to solving the scattering problem in a material with many small particles embedded in it help to understand better the dependence of the effective field in the material on the basic parameters of the problem, namely, on a , M , d , ζ_m , $N(x)$, and $h(x)$.

The accuracy of the solution to the limiting equation (9) depends on the values of k , a , and on the function $h(x)$. The accuracy of the solution improves as the number P increases. The relative error of the solution to asymptotic LAS (15) depends essentially on the function $N(x)$ which is at our disposal. In our numerical experiments $N(x) = \text{const}$. The accuracy of the solution is improved if $N(x)$ decreases. The error of the solution decreases if M grows. The relative difference between the solutions to LAS (15) and (16) can be improved by changing the distance d between the particles, a being fixed. The optimal values of d change slowly in the considered range of function $N(x)$. The relative error is smaller for smaller a .

The numerical results demonstrate a possibility to apply the proposed technique for investigation of the properties of materials with defects. The refraction coefficient n^2 of defect media depends on the radius a of particle and distance d between them.

1. <http://www.polytec.com/us/products/vibration-sensors/single-point-vibrometers/modular-systems/ofv-5000-modular-vibrometer-controller/>.
2. Ramm A.G. *Wave scattering by Small Bodies of Arbitrary Shapes*. World Scientific, Singapore, 2005.
3. Ramm A.G. *Inverse Problems*. Springer, Berlin, 2005.
4. Ramm A.G. *Many Body Wave Scattering by Small Bodies and Applications // J. Math. Phys.* – Vol. 48, No 10, 2007, 103511.
5. Ramm A.G. *Wave Scattering by Many Small Particles Embedded in a Medium // Physics Letters A*, 372, 2008. – P. 3064–3070.
6. Ramm A.G. *A Collocation Method for Solving Integral Equations // Intern. Journ. of Comput. Sci. and Mathem.* – Vol. 3, No 2, 2009. – P. 222–228.
7. Zhitlukhina Y. V., Perov D. V., Rinkevich A. B., Permikin V. S. *Detection of the microdefects in metals on the basis of study of the acoustic fields // Defectoscopy*, No 10, 2007. – P. 26–40. (in Russian).
8. Andriychuk M. I., Ramm A.G. *Scattering by many small particles and creating materials with a desired*

refraction coefficient // International Journal of Computing Science and Mathematics. – Vol. 3, Nos.1/2, 2010. – P. 102–121. 9. Andriychuk M.I., Ramm A.G. Numerical Solution of Many-Body Wave Scattering Problem for Small Particles and Creating Materials with Desired Refraction Coefficient // In book Numerical Simulations of Physical and Engineering Processes. Ed. by Jan Awrejcewicz, InTech, Rieka, 2011. – P. 3–28.

UDK 519.1:656

L. Bugada, V. Tkachuk

O. S. Popov Odessa National Academy of Telecommunications

QUESTIONS ON OPTIMIZATION OF TRUNK MAIL TRANSPORTATION

© Bugada L., Tkachuk V., 2012

The questions of optimization of the number and total length of trunk mail postal routes and grounded optimized schemes of trunk mail transportation have been considered.

Key words: postal communications, trunk mail transportation, postal establishments, letter-post.

Розглянуто питання оптимізації кількості та загальної довжини магістральних поштових маршрутів і наземних оптимізованих схем магістралей поштових перевезень.

Ключові слова: поштовий зв'язок, магістральне перевезення пошти, поштові організації, письмова кореспонденція.

Introduction

The purpose of postal communications appears to dramatically reduce of costs on the postal network functioning, to enhance the quality of postal services, to improve the competitiveness of the national postal operator of Ukraine.

One of the main directions of development of technical and technological post infrastructure is to reduce the costs of handling and transportation of mail by the creation one or more sorting postal establishments (PE) in which there are concentrated large postal flows and provided prerequisites of implementation of automatic mail processing and efficient use of vehicles for mail transportation [1].

The basis of postal network functioning is trunk transportations. Since the trunk mail transportation are carried out between sorting PE, optimization of the number and location of sorting PE is primary, and optimization of trunk mail transportation scheme is on secondary priority. It is necessary to determine the number and location of sorting PE in order to optimize trunk mail transportation.

By resolving this logistics problem it should simultaneously take into account the number of handling mail locations, the number and length of routes.

Trunk postal network is one of the main parts of a single postal network of Ukraine, which provides a steady and regular postal communications of main hub (Kyiv) with all regional centers and via regional centers.

The main bulk of postal items is transported on trunk postal routes (almost all periodicals, most of the parcels, and also the bulk of international postal items). Therefore, the rational organization of the trunk postal communications affects on organization of postal communications in general, the quality and efficiency of its work.

Today, letter post (LP) sorting holds in each region of Ukraine, objects for sorting are 25, that use 37 postal routes (except routes for express mail, international routes) accordingly.

To reduce the costs of mail processing, Science research centre "Index" of O. S. Popov ONAT was proposed to enhance regional sorting centers (RSC) with manual sorting of LP on the basis of existing PE